

# A mathematical model of the hypothalamic network controlling the pulsatile secretion of reproductive hormones

Margaritis Voliotis<sup>1,2,\*</sup>, Xiao Feng Li<sup>3</sup>, Kevin T. O’Byrne<sup>3</sup>, Krasimira Tsaneva-Atanasova<sup>1,2,\*</sup>,

**1** Department of Mathematics and Living Systems Institute, College of Engineering, Mathematics and Physical Sciences, University of Exeter, Exeter, EX4 4QF, UK

**2** EPSRC Centre for Predictive Modelling in Healthcare, University of Exeter, Exeter, EX4 4QJ, UK.

**3** Department of Women and Children’s Health, School of Life Course Sciences, King’s College London, London SE1 1UL, UK.

\* M.Voliotis@exeter.ac.uk, K.Tsaneva-Atanasova@exeter.ac.uk

## Abstract

Reproduction critically depends on the pulsatile secretion of gonadotrophin-releasing hormone (GnRH) from the hypothalamus. This ultradian rhythm drives the secretion of gonadotrophic hormones (LH and FSH) from the pituitary gland, which are critical for gametogenesis and ovulation, and its frequency is regulated throughout the life course to maintain normal reproductive health. However, the precise mechanisms controlling the pulsatile GnRH dynamics are unknown. Here, we propose and study a novel mathematical model of a population of neurones in the arcuate nucleus (ARC) of the hypothalamus that co-expresses three key modulators of GnRH secretion: kisspeptin; neurokinin B (NKB); and dynorphin (Dyn). The model highlights that positive feedback in the population exerted by NKB and negative feedback mediated by Dyn are the two key components of the pulse generator, which operates as a relaxation oscillator. Furthermore, we use the model to study how external inputs modulate the frequency of

the pulse generator, a prediction that can be readily tested in-vivo using optogenetically-driven stimulation. Finally, our model predicts the response of the system to various neuropharmacological perturbations and reconciles inconsistent experimental observations following such interventions in-vivo. We anticipate that our model in combination with cutting-edge, in-vivo techniques, allowing for neuronal stimulation and recording, will set the stage for a quantitative, system-level understanding of the GnRH pulse generator.

## Introduction

Reproduction is fundamental for the survival of species and is therefore tightly regulated even in the simplest of living organisms. In mammals, reproduction is controlled by the coordinated action of the brain, the pituitary gland, and the gonads. Within the brain a neuronal clock drives the periodic release of gonadotrophin-releasing hormone (GnRH). The operation of this GnRH pulse generator at a frequency appropriate for the species is critical for the generation of gonadotrophin hormone signals (luteinizing hormone, LH; and follicle-stimulating hormone, FSH) by the pituitary gland, which stimulate the gonads and set in motion gametogenesis and ovulation. However, the mechanisms underlying the GnRH pulse generator remain poorly understood.

GnRH is produced from specialised neurones, known as GnRH neurones, and its secretion into the pituitary is controlled by upstream hypothalamic signals [1]. Neuropeptide kisspeptin has been identified as a key regulator of GnRH as both humans and rodents with inactivating mutations in kisspeptin or its receptor fail to progress through puberty or show normal pulsatile LH secretion [2–4]. Within the hypothalamus, two major kisspeptin producing neuronal populations are located in the arcuate nucleus (ARC) and in the preoptical area [5] or the anteroventral periventricular (AVPV)/rostral periventricular (PeN) continuum in rodents [6]. Moreover, the invariable association between neuronal activity in the ARC and LH pulses across a range of species from rodents to primates [7] has been suggestive that the ARC is the location of the GnRH pulse generator, and therefore the ARC kisspeptin neurones, also known as KNDy for co-expressing neurokinin B (NKB) and dynorphin (Dyn) alongside kisspeptin [8], constitute the core of the GnRH pulse generator.

Although animal studies have shown that the KNDy population plays a critical role 24  
in the regulation of GnRH, there has been relatively little information on the regulatory 25  
mechanisms involved in generating and sustaining pulsatile dynamics. Pharmacological 26  
modulators of kisspeptin, NKB and Dyn signalling have been extensively used to perturb 27  
the system and study the effect on the activity of the neuronal population (using 28  
hypothalamic multiunit activity (MUA) volleys as a proxy), as well as on downstream 29  
GnRH/LH dynamics [9–12]. For example, it has been shown that kisspeptin (Kp-10) 30  
administration does not affect MUA volleys in the ovariectomised rat [9], suggesting 31  
that kisspeptin is relaying the pulsatile signal to GnRH neurones rather than generating 32  
it. On the contrary, administration of NKB or Dyn modulates MUA volley frequency 33  
in the ovariectomised goat [11], suggesting a more active role for these neuropeptides 34  
in the generation of the pulses. Deciphering, however, the role of NKB has been 35  
problematic, and there exist conflicting data showing either an increase or decrease of 36  
LH levels in response to administration of a selective NKB receptor agonist (senktide) 37  
[10, 12, 13]. Recently, a study combining optogenetics, with whole-cell electrophysiology 38  
and molecular pharmacology has shed light on the action of neuropeptides NKB and 39  
Dyn and their role in controlling reproductive function [14]. The key mechanistic insight 40  
from this study was that NKB functions as an excitatory signal by depolarising cells at 41  
the post-synaptic end, while Dyn functions as an inhibitory signal by suppressing the 42  
action of NKB at the presynaptic end. 43

Here, motivated by these experimental findings, we develop a mathematical model of 44  
the ARC KNDy population. The model is based on a network description of the popula- 45  
tion and captures two important processes: secretion of Dyn and NKB by individual 46  
neurones; and regulation of the population firing activity by the two neuropeptides. The 47  
model predicts that the KNDy population can indeed generate and sustain oscillatory 48  
firing dynamics similar to the multi-unit activity (MUA) volleys observed in-vivo [12] 49  
and provides insight on mechanism underlying pulse generation. Furthermore, our model 50  
predicts the response of the system to various neuropharmacological perturbations and 51  
reconciles inconsistent experimental observations following such interventions in-vivo. 52  
Finally, we perform global sensitivity analysis to uncover possible pathways through 53  
which the dynamics of the system can be modulated. Our model complements existing 54  
phenomenological models of GnRH dynamics [15], and makes testable in-vivo predictions 55

that will shed light on the mechanisms underlying GnRH regulation.

## Results

### A mathematical network model describing the ARC KNDy population

We use a mathematical network model (Fig 1A) to describe and study the collective dynamics of KNDy neurones in the ARC. The model describes the dynamics of  $M$  synaptically connected KNDy neurones using a set of coupled ordinary differential equations (ODEs). For each neurone  $i$ , we use variables  $D_i$  and  $N_i$ , to denote the concentration of Dyn and NKB, secreted at its synaptic ends; and variable  $v_i$  to denote its firing rate, measured in spikes/min. The ODEs describing the dynamics of neurone  $i$  in the population are:

$$\frac{dD_i}{dt} = f_D(v_i) - d_D D_i; \quad (1)$$

$$\frac{dN_i}{dt} = f_N(v_i, D_i) - d_N N_i; \quad (2)$$

$$\frac{dv_i}{dt} = f_v\left(\{v_j, N_j\}_{j \in \text{neigh}(i)}\right) - d_v v_i. \quad (3)$$

Parameters  $d_D$ ,  $d_N$  and  $d_v$  prescribe the characteristic timescale for each variable. In particular, parameters  $d_D$  and  $d_N$  correspond to the rate at which Dyn and NKB are lost (e.g., due to diffusion or active degradation), while  $d_v$  relates to the rate at which neuronal activity resets to its basal level. Functions  $f_D$ ,  $f_N$  give the secretion rate of Dyn and NKB, respectively, while function  $f_v$  encodes how the firing rates changes in response to synaptic inputs. Crucially, the activity of neurone  $i$ ,  $v_i$ , depends on the firing rate and secreted level of NKB of all other neurones  $j$  that are synaptically connected to it. This dependence is denoted by the curly brackets notation in the arguments list of  $f_v$ . Synaptic connections are summarised by the adjacency matrix,  $A$ : a binary, square ( $M \times M$ ) matrix with  $A_{ij} = 1(0)$  indicating synaptic connectivity from neurone  $i$  to neurone  $j$ . In the model, synaptic connections are formed randomly between all neurones with a constant probability, i.e.,  $\text{Prob}(A_{ij} = 1) = \bar{c}$ .

We use the following sigmoidal (Hill-type) functions to describe regulatory relation-

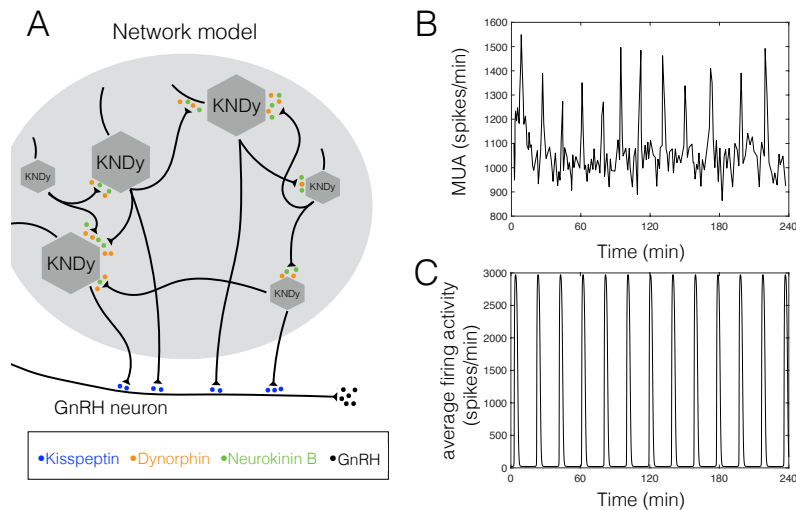


**Fig 1. A network model of KNDy neurones in the arcuate nucleus (ARC).** (A) Schematic illustration of the dynamical, network model comprising a population of synaptically connected KNDy neurones. In the model, the neuronal firing rate drives the secretion of regulatory neuropeptides dynorphin (Dyn) and neurokinin B (NKB). Furthermore, NKB excites postsynaptic neurones while Dyn inhibits NKB secretion pre-synaptically. (B) Multi-unit activity (MUA) volleys recorded from the hypothalamus of an ovariectomized rat (data from [12]). (C) The model produces sustained oscillations with explosive spikes of neuronal activity similar to those observed in-vivo. Model parameters were inferred from the data in (B) using an Approximate Bayesian Computation method based on sequential Monte Carlo (ABC SMC; see Material and Methods section) and are listed in Tbl 1.

ships between the variables. In particular, we set the the secretion rate of Dyn and NKB to be:

$$f_D(v) = k_D \frac{v^{n_1}}{v^{n_1} + K_{v,1}^{n_1}};$$

$$f_N(v, D) = k_N \frac{v^{n_2}}{v^{n_2} + K_{v,2}^{n_2}} \frac{K_D^{n_3}}{D^{n_3} + K_D^{n_3}}.$$

That is, neuronal activity stimulates secretion of both neuropeptides, and Dyn represses NKB secretion, which is in agreement with experimental evidence of Dyn inhibiting the action of NKB presynaptically [14]. Neuropeptides secretion is limited by the available neuropeptide pools as well as by other biochemical species driving or regulating the process, therefore in the model we allow saturation of the secretion rate above certain thresholds of  $v$  and  $D$ , which are set by parameters  $K_{v,1}$ ,  $K_{v,2}$  and  $K_D$ . Furthermore,

we set

$$f_v \left( \{v_j, N_j\}_{j \in \text{neigh}(i)} \right) = v_0 \left( \frac{2}{\exp(-I) + 1} - 1 \right); I = I_0 + \sum_{j \in \text{neigh}(i)} p_v \frac{N_j^{n_4}}{N_j^{n_4} + K_N^{n_4}} v_j,$$

where  $v_0$  is the maximum rate at which the firing rate increases in response to synaptic 72  
inputs. The stimulatory effect of NKB (secreted at the presynaptic end) is mediated via 73  
G protein-coupled receptor Tacr3 and is manifested as a short-term depolarisation of 74  
the postsynaptic neurone [14]. In our equation above, we accommodate this effect by 75  
letting the synaptic strength be a function of the secreted NKB. Moreover, parameter 76  
 $p_v$  sets the maximum strength of the synapse, while parameter  $K_N$  sets the level of 77  
NKB at which its effect is half-maximal. Finally, parameter  $I_0$  captures synaptic inputs 78  
stemming from other neuronal populations or from synaptic noise. 79

We infer model parameters using the frequency and duty-cycle of the multi-unit 80  
activity (MUA) volleys recorded from the hypothalamus of an ovariectomized rat [12] (see 81  
Material and Methods section). As illustrated in Fig 1B&C, the model can replicate 82  
pulses of synchronised activity similar to the MUA signal recorded in-vivo. This finding 83  
further supports the hypothesis that KNDy neurones in the ARC constitute the core 84  
of the GnRH pulse generator. Furthermore, the model will allow us to study the 85  
mechanisms generating and sustaining the rhythmic activation of the KNDy neural 86  
network, facilitating our understanding of the relationships underpinning this complex 87  
biological system. 88

## A relaxation oscillator drives the pulsatile activity of the KNDy 89 neuronal population 90

Having shown that the model can reproduce sustained pulses of neuronal activity (see 91  
Fig 1B), we move to study the mechanisms driving the phenomenon. To do so, we 92  
simplify the network model, and derive a coarse-grained (mean-field) model of the 93  
neuronal population comprising three dynamical variables:  $\bar{D}$ , representing the average 94  
concentration of Dyn secreted;  $\bar{N}$ , representing the concentration of NKB secreted; and 95  
 $\bar{v}$ , representing the average firing activity of the neuronal population. Derivation of 96  
the coarse-grained model proceeds by averaging Eq 3 over all neurones (index  $i$ ); and 97

expanding (keeping up to leading term) all non-linear functions of  $D_i$ ,  $N_i$  and  $v_i$  around the population-averaged values,  $\bar{D} = \sum_i D_i/M$ ,  $\bar{N} = \sum_i N_i/M$  and  $\bar{v} = \sum_i v_i/M$  (see S1 text). The resulting equations, describing the time evolution of the population-averaged variables, are:

$$\frac{d\bar{D}}{dt} = f_D(\bar{v}) - d_D\bar{D}; \quad (4)$$

$$\frac{d\bar{N}}{dt} = f_N(\bar{v}, \bar{D}) - d_N\bar{N}; \quad (5)$$

$$\frac{d\bar{v}}{dt} = f_v(\bar{v}, \bar{N}) - d_v\bar{v}. \quad (6)$$

All parameters and functions are defined as before (see section above), except for synaptic input  $I$  that now takes the form:  $I = I_0 + p_v\bar{c}M \frac{\bar{N}^{n_4}}{\bar{N}^{n_4} + K_N^{n_4}}\bar{v}$ , where  $\bar{c}$  is the average number of synapses that a neurone receives as a fraction of the population size. 91 92 93

To explore the mechanisms underpinning the oscillatory behaviour, we remove Dyn-mediated negative feedback from the system and study the the dynamics of the  $(\bar{N}, \bar{v})$  subsystem treating variable  $\bar{D}$  as a bifurcation parameter. The result of this analysis is illustrated in Fig 2B and shows that for intermediate values of Dyn the  $(\bar{N}, \bar{v})$  exhibits two stable steady states corresponding to the high and low branches shown in Fig 2B. This bistable behaviour, stemming from the non-linear, positive feedback between neuronal activity and NKB secretion, leads to sustained oscillations of neuronal activity when combined with slow negative feedback mediated through Dyn. Furthermore, we expect exogenous inhibitory/excitatory sources, such as distinct neuronal populations or synaptic noise, to be direct modulators of the oscillatory behaviour by altering the dynamic behaviour of the  $(\bar{N}, \bar{v})$  sub-system. Indeed, treating the basal synaptic inputs parameter,  $I_0$ , as a bifurcation parameter, we find that oscillatory behaviour of the system is limited to a critical range. In particular, as inputs are increased from zero, high-amplitude, low-frequency pulses emerge after a homoclinic bifurcation (Fig 2C; HC point). The value of  $I_0$  at which the bifurcation occurs is equivalent to driving the neuronal population at a rate of approximately 0.024 Hz in the absence of NKB and Dyn modulation. As external excitation ramps up, the frequency of pulses continues to increase, until oscillations disappear altogether through a Hopf bifurcation (Fig 2C; HB point) and the system re-enters a mono-stable regime. In engineering terms, the system 94 95 96 97 98 99 100 101 102 103 104 105 106 107 108 109 110 111 112

behaves as a relaxation oscillator, where the bi-stable subsystem is successively triggered 113  
 by external excitation and silenced due to negative feedback. We should note that a 114  
 sufficiently slow negative feedback can sustain oscillations in the absence of bistability, 115  
 however, the combination of bistability with negative feedback is a recurring motif in 116  
 many biological oscillators [16, 17]. 117

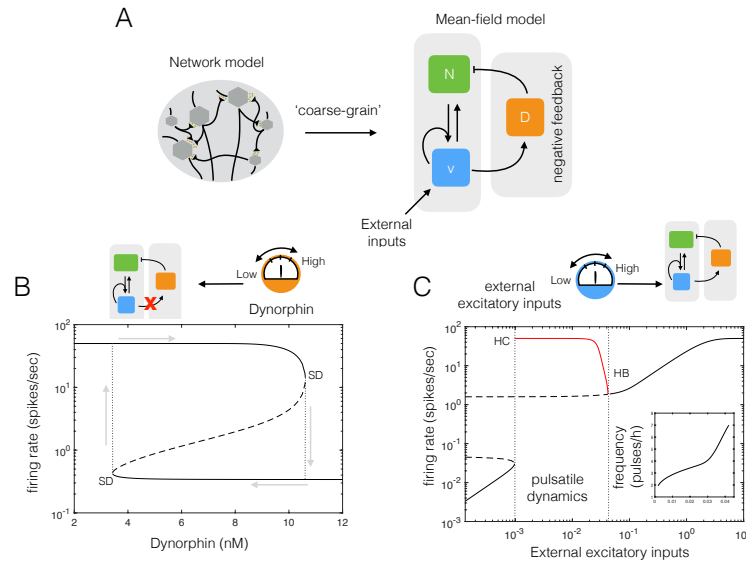


**Fig 2. A coarse-grained model gives mechanistic insight into the pulsatile behaviour of the neuronal population.** (A) We simplify the network model by deriving a mean-field model of the neuronal population comprising three dynamical variables:  $\bar{D}$ , representing the average concentration of Dyn secreted;  $\bar{N}$ , representing the concentration of NKB secreted; and  $\bar{v}$ , representing the average firing activity of the neuronal population. (B) After disrupting the negative feedback loop (i.e., setting Dynorphin under external control) the system exhibits, for intermediate values of Dynorphin, two stable steady-states (upper and lower solid lines) and an unstable one (dashed line). At the edges of the bistable regime equilibria are lost through a saddle-node bifurcation (SD points). The bistability gives rise to hysteresis as the value of Dyn is varied externally (grey arrows). (C) The coarse-grained model predicts how external excitatory inputs affect the system's dynamics and pulse frequency. As external excitation is increased from zero, high-amplitude, low-frequency pulses emerge after some critical value (HC point; homoclinic bifurcation). The frequency of pulses continues to increase with external excitation until oscillations disappear altogether (HB point; Hopf bifurcation) and the system enters a mono-stable regime. Model parameter values are given in Tbl 1.



**The model predicts the response of the system to various neuro- 118  
pharmacological perturbations and reconciles inconsistent ex- 119  
perimental observations following such interventions in-vivo 120**

Neuropharmacology is a powerful tool used to study the role of neurotransmitter and neu- 121  
ropeptide signalling on the pulsatile GnRH dynamics. In-vivo, localised administration 122  
of drugs that selectively activate or inhibit certain pathways of interest, can shed light 123  
on the regulatory mechanism underlying pulse generation and frequency modulation. 124  
However, the effect of such neuropharmacological perturbations can appear confusing 125  
and difficult to interpret when feedback interactions and non-linearities are present in 126  
the system. One notable example, regards senktide (a selective NKB receptor agonist) 127  
that appears to be suppressing pulsatile GnRH/LH dynamics in some cases [12, 13] while 128  
stimulating LH secretion in others [10]. To study this controversial finding, we extend 129  
our coarse-grained model to accommodate the effect of two drugs often used to perturb 130  
the system in-vivo: senktide, a selective NKB receptor agonist; and nor-BNI, a selective 131  
 $\kappa$ -opioid receptor antagonist. We use  $E$  to denote the drug concentration injected into 132  
the system. As senktide has the same effect as NKB but functions independently, we 133  
incorporate it in our model by modifying the expression for the synaptic input  $I$  as 134  
follows: 135

$$I = I_0 + p_v \bar{c} M \frac{\bar{N}^{n_4} + E^{n_4}}{\bar{N}^{n_4} + E^{n_4} + K_N^{n_4}} \bar{v}$$

On the other hand, nor-BNI blocks Dyn signalling, therefore we modify function  $f_N$  to 136  
read: 137

$$f_N(v, D) = k_N \frac{v^{n_2}}{v^{n_2} + K_{v,2}^{n_2}} \frac{K_D^{n_3} + E^{n_3}}{D^{n_3} + E^{n_3} + K_D^{n_3}}.$$

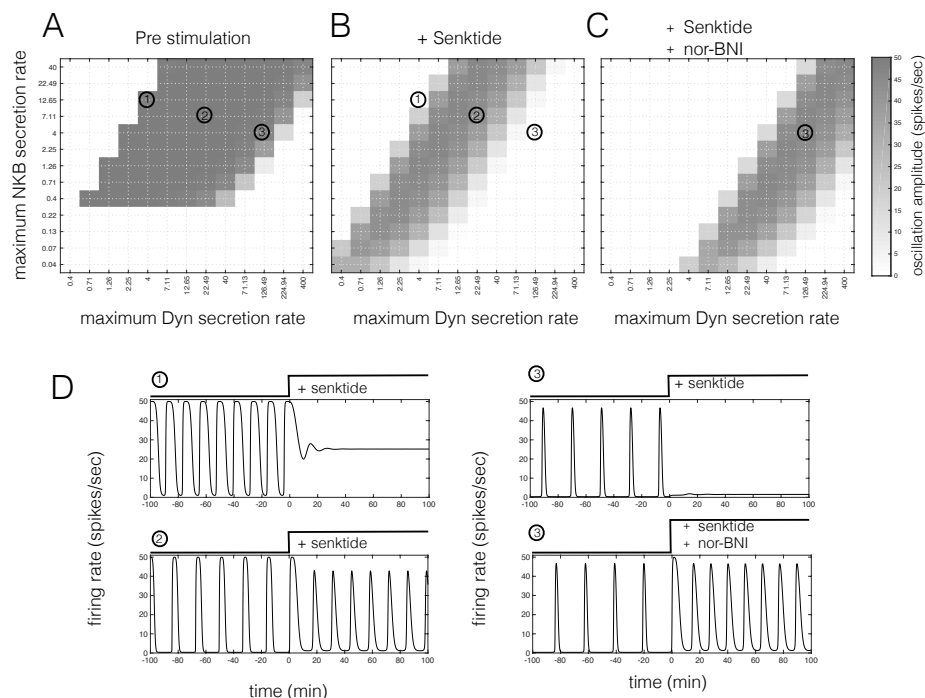
That is, the antagonist is effectively increasing parameter  $K_{v,2}$  in the model. 138

Figure 3A&B illustrates that the effect of perturbing the system with senktide varies 139  
depending on the underlying NKB and Dyn secretion capacity (parameters  $k_N$  and  $k_D$  140  
in the model). In particular, Fig 3A shows the region over the parameter space (grey 141  
area) for which the unperturbed system demonstrates pulsatile dynamics. This region 142  
is deformed after senktide administration, and given the system starts from within the 143  
oscillatory regime three distinct response types are observed (see Fig 3B; indicative 144  
examples are marked with numbers). First, administration of senktide can set the system 145

in a steady-state of elevated activity after a transient spike (see trace marked 1). Such  
an effect is consistent with data from diestrus rats, showing that intracerebroventricular  
administration of senktide to gonadal intact rats in the diestrous phase of the estrous  
cycle stimulated transiently LH secretion [12]. Second, administration of senktide can  
increase the pulse frequency (see trace marked 2 and Fig C in S1 text). This type of  
response is consistent with data showing that intracerebroventricular administration of  
NKB increases the frequency of multiunit electrical activity (MUA) volleys recorded  
from the medial basal hypothalamus in the OVX goat [11]. An increase in the frequency  
of MUA volleys in response to central nor-BNI administration [11] is also in agreement  
with the model (see Fig B in S1 text). Finally, administration of senktide can suppress  
pulsatile dynamics setting the system in a low activity steady-state (see trace marked 3).  
This apparent inhibition of the system through an excitatory agent although counter  
intuitive is in agreement with the inhibition of hypothalamic MUA volleys and serum LH  
observed in adult OVX rats after intracerebroventricular administration of senktide [12].  
Fig 3C illustrates the effect of perturbing the system with a combination of NKB and  
nor-BNI. Note, that the combined administration of the two drugs can preserve pulsatile  
dynamics in cases where senktide alone was suppressing it (see trace 3); in agreement  
with experimental data showing that nor-BNI blocks the senktide-induced suppression  
of pulsatile LH secretion in OVX rats [12].

## **Global sensitivity analysis predicts robustness of oscillatory behaviour to parameter perturbation**

The dynamics of GnRH secretion are tightly controlled throughout life, from the initial  
stages of postnatal development and throughout adulthood [1]. However, the specific  
pathways through which control is achieved remain mostly unknown. Here, we use  
the model and global sensitivity analysis to study how various factors could affect the  
dynamic behaviour of the KNDy population in the arcuate nucleus and hence GnRH  
secretion. We restrict our focus to three model parameters: the maximum Dyn secretion  
rate,  $k_D$ ; the maximum NKB secretion rate  $k_N$ ; and the magnitude of basal synaptic  
inputs,  $I_0$ . Variability in  $k_D$  and  $k_N$  capture, for example, regulation of Dyn and  
NKB levels by sex steroids during menstrual/oestrous cycle [18], whereas changes in



**Fig 3. The effect of neuropharmacological perturbations on the activity of the KNDy population.** Perturbation of the system with two drugs: senktide, a selective NKB receptor agonist; and nor-BNI, a selective Dyn receptor antagonist. The effect of the perturbation on the dynamics depends on the NKB and Dyn secretion rate. (A) The magnitude of oscillations (grey scale) in the unperturbed system for different levels of maximum NKB and Dyn secretion rate (parameters  $k_N$  and  $k_D$  in the model). (B) The magnitude of oscillations after perturbing the system with senktide ( $E_{senktide} = 60$  pM). (C) The magnitude of oscillations after perturbing the system with senktide ( $E_{senktide} = 60$  pM) and nor-BNI ( $E_{nor-BNI} = 4.1$  nM) simultaneously. (D) Time-traces of the system activity in response to neuropharmacological perturbations with senktide and nor-BNI. Time-traces correspond to the  $(k_N, k_D)$  combinations marked in (A)-(C).

$I_0$  could map to changes in the excitatory/inhibitory inputs the population receives in developmental stages [1]. To understand how changes in these three parameters affect system dynamics, we vary them independently over a wide range (see Material and Methods section) and study how parameter variability accounts for variance in various critical features of the system's dynamics, e.g., amplitude and period of oscillations.

In Fig 4A, the first order sensitivity indices indicate the proportion of variance of a response feature that is explained by variation in a parameter, while keeping the remaining parameters fixed. First order sensitivity indices, therefore, quantify the effect that single parameter perturbations have on the dynamics of the system. We find that the amplitude of oscillations is most sensitive to changes in the external synaptic

inputs ( $I_0$ ), and that the maximum magnitude of the response is sensitive to changes 186  
in the maximum Dyn secretion rate ( $k_D$ ). Also, the period of oscillations appears 187  
robust to changes in any of the three parameters in isolation. Fig 4B reports the total 188  
order sensitivity indices, that is the proportion of variance in a response feature that is 189  
explained by variation in a parameter, while allowing other parameters to vary as well. 190  
Therefore, the total order sensitivity index of a parameter is a proxy for the effect this 191  
parameters has on the dynamics of the systems when co-varied with other parameters. 192  
We find that the amplitude as well as the period of oscillations is far more sensitive 193  
to combined changes of the parameters. For example, 28% of the total variance in the 194  
amplitude of oscillations is attributable to variation of  $I_0$  alone, whereas this figure 195  
jumps to more than 76% when variations in other parameters is taken into consideration. 196  
Similarly, approximately 83% of the variance in the period of oscillations is explained 197  
when parameters are allowed to covary, compared to no more than 14.5% when single 198  
parameter variation is considered. 199

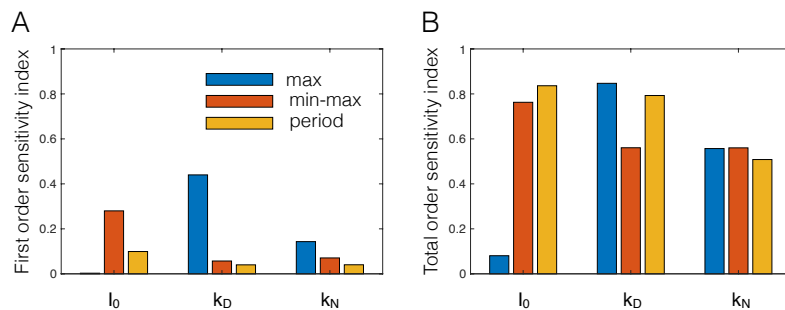


**Fig 4. Global sensitivity analysis of the coarse-grained model.** Global sensitivity analysis of the coarse-grained model considering maximum response amplitude, minimum response amplitude, amplitude of oscillations, and period of oscillations. First order (A) and total-order (B) sensitivity indices are shown for parameters  $k_D$  (maximum rate of Dyn secretion),  $k_N$  (maximum rate of NKB secretion) and  $I_0$  (magnitude of external synaptic inputs).

## Discussion and Conclusions

Motivated by recent experimental evidence, we developed and studied a mathematical 201  
model of the KNDy population in the arcuate nucleus, a population that has been 202  
shown to be critical for GnRH pulsatile dynamics [19]. Our model demonstrates that the 203  
KNDy population can indeed produce and sustain pulses of neuronal activity that drive 204

GnRH secretion. The system works as a relaxation oscillator. On the one hand, external 205  
excitation and auto-stimulation via NKB signalling effectively allows the population 206  
to behave as a bistable switch, firing either at a high or low rate. Moreover, negative 207  
feedback through Dyn signalling allows the population to switch between the two activity 208  
states in a regular manner, giving rise to pulses of neuronal activity. We found that 209  
this mechanism of pulse generation is robust to parameter perturbations. In fact, co- 210  
variation of parameters governing, for example, the magnitude of external inputs, and 211  
the maximum secretion rates of NKB and Dyn is a more effective way of modulating 212  
the systems' oscillatory behaviour (amplitude and frequency). This multi-channel mode 213  
of efficient regulation is perhaps not surprising given the system's crucial function, and 214  
hints that steroid feedback modulating the dynamics of the pulse generator over the 215  
reproductive cycle in female mammals is mediated through multiple, possibly interlinked, 216  
pathways. 217

The proposed model allowed us to study the effect of pharmacological modulators 218  
of NKB and Dyn signalling. We find that NKB receptor agonists, such as senktide, 219  
could have either an inhibitory or an excitatory effect on the dynamics of the model. 220  
We show that this response variability can be explained, for example, by variation in 221  
parameters that control the levels of Dyn and NKB secreted by the neurones, which in- 222  
vivo are controlled by the sex-steroid milieu. This finding reconciles previous conflicting 223  
evidence regarding the effect of senktide on the levels of LH secretion [10, 12, 13]. Our 224  
results also highlight the need for a more quantitative understanding of how the sex- 225  
steroid milieu affects the NKB and Dyn signalling pathways in the KNDy population. 226  
Such an understanding will lead to more accurate interpretation of results from in-vivo 227  
neuropharmacological perturbation experiments in various animal models and will shed 228  
light on the mechanisms underlying the regulation of GnRH pulsatile secretion. 229

Furthermore, the model makes a series of testable predictions. First, the model 230  
predicts that pulsatile dynamics of the system critically depend on external excitatory 231  
or inhibitory signals that the KNDy population receives. For example, low external 232  
excitation should silence the system, whereas high excitation should fix the system 233  
on a high activity state. This can be tested in-vivo using optogenetics [20–22], that 234  
is, by introducing light-sensitive ion-channels into the KNDy neurones and using light 235  
to continuously activate or inhibit them, one should be able to directly control 236

the generation and frequency of pulses. Moreover, the model predicts that the auto- 237  
stimulatory effect of NKB signalling leads to bistable dynamics (see Fig 2B), a property 238  
that allows the system to function as a relaxation oscillator [16,17]. Therefore, disrupting 239  
the Dyn-mediated negative feedback should leave the system either at a low or high 240  
activity state depending on the timing of the disruption relative to the period of the 241  
oscillation (see Fig D in S1 text). Testing such predictions will be critical for our 242  
understanding of the fundamental dynamic mechanisms governing the GnRH pulse 243  
generator behaviour. 244

Finally, the model can be extended to incorporate the effect of sex hormones, for 245  
example, by explicitly modelling circulating concentrations of sex hormones and allowing 246  
them to modulate parameters of the current model (e.g., those governing the maximum 247  
and minimum secretion rate of NKB and Dyn). This would be a step towards a 248  
comprehensive mathematical model that reliably replicates hormonal dynamics in the 249  
reproductive axis over longer timescales, spanning, for example, the menstrual/oestrous 250  
cycle. We envision that as hormonal measurement techniques advance, enabling accurate, 251  
real-time readouts from individuals at low cost, such predictive mathematical models 252  
would be a valuable tool to the personalised design of IVF protocols and hormonal 253  
contraception methods. 254

## Materials and methods 255

### Bifurcation analysis and numerical experiments 256

Bifurcation analysis of the coarse-grained model was performed using AUTO-07p [23]. 257  
Both the full network model and coarse-grained model were simulated in Matlab using 258  
function ode45 (explicit Runge-Kutta (4, 5) solver). 259

### Parameter inference 260

Parameter inference was performed using an Approximate Bayesian Computation (ABC) 261  
method based on sequential Monte Carlo (SMC) [24]. In ABC SMC a population of 262  
parameter vectors or particles,  $\theta$ , is initially sampled from the prior distribution  $\pi_0$  and 263  
propagated with the use of a perturbation kernel through a sequence of distributions 264

$\pi_i, i = 1, \dots, \mathcal{T}$ . The final distribution  $\pi_{\mathcal{T}}(\theta|d(x, x^*) < \epsilon_{\mathcal{T}})$  corresponds to the (approximate) target posterior distribution, where  $d(x, x^*)$  is the distance function comparing the simulated dataset  $x^*$  to the experimental data  $x$  and  $\epsilon_{\mathcal{T}}$  is the final error tolerance level. Intermediate distributions are associated with a series of decreasing tolerance levels  $\epsilon_i, i = 1, \dots, \mathcal{T} - 1$ , making the transition to  $\pi_{\mathcal{T}}$  more gradual and avoiding getting stuck in areas of low probability.

Here, to ensure gradual transition between populations we take  $\mathcal{T} = 21$  and set tolerance levels to  $\epsilon_i = 10^{(1-0.2i)}, i = 1, \dots, \mathcal{T}$ . The size of each population is set to 500 particles. For each particle, the activity of the KNDy is simulated from  $t = 0$  to 6000min, the first 1000 min are discarded, and the remaining time-trace is used to calculate the pulse frequency and duty cycle (defined as the fraction of one period in which KNDy activity is above 50% of the pulse amplitude). The distance function,  $d$ , is defined as the sum of the squared relative error in these two summary statistics between the simulated dataset and the data (see Fig 1A; frequency 3.12 pulses/hour; duty cycle 0.15). The prior parameter distributions were chosen as follows:  $\log_{10}(d_D) \sim \mathcal{U}(-2, 1)$ ;  $\log_{10}(d_N) \sim \mathcal{U}(-2, 1)$ ;  $\log_{10}(d_v) \sim \mathcal{U}(0, 2)$ ;  $\log_{10}(k_D) \sim \mathcal{U}(-1, 3)$ ;  $k_N \sim \mathcal{N}(40, 4)$  estimate from [25] plus 10% error;  $\log_{10}(p_v) \sim \mathcal{U}(-3, 1)$ ;  $K_D \sim \mathcal{N}(0.3, 0.03)$  estimate from [26] plus 10% error;  $K_N \sim \mathcal{N}(4, 0.4)$  estimate from [27] plus 10% error;  $K_{v,1} \sim \mathcal{U}(1, 3)$ ;  $K_{v,2} \sim \mathcal{U}(1, 3)$ ;  $\log_{10}(I_0) \sim \mathcal{U}(-3, 0)$ ; where  $\mathcal{U}(min, max)$  denotes the uniform distribution in the interval  $[min, max]$ , and  $\mathcal{N}(\mu, \sigma)$  denotes the normal distribution with mean,  $\mu$ , and standard deviation,  $\sigma$ . For parameters  $k_N, K_D, K_N, K_{v,1}$ , and  $K_{v,2}$  gaussian perturbation kernels were used with standard deviation 4, 0.03, 0.4, 10 and 10 respectively. For all remaining parameter log-normal perturbation kernels were used with standard deviation 0.05. An (approximate) maximum a posteriori (MAP) estimate of model parameters (corresponding to the parameter values of to the most probable particle in the final population) is given in Tbl 1. Histograms of the approximate marginal posterior distribution of each parameter and pairwise scatter plots are shown in Fig A in S1 text.

## Global sensitivity analysis

Global sensitivity analysis was performed in Matlab using eFast [28]. For each parameter set, the model was initialised randomly and run from  $t = 0$  to 6000 min. Response

**Table 1.** Model parameters. An (approximate) maximum a posteriori (MAP) estimate of the model parameters obtained using an Approximate Bayesian Computation method based on sequential Monte Carlo (ABC SMC).

No.	Parameter	Description	Value
1	$M$	Population size	1000 cells
2	$d_D$	Dyn degradation rate	$0.367 \text{ min}^{-1}$
3	$d_N$	NKB degradation rate	$0.351 \text{ min}^{-1}$
4	$d_v$	firing rate reset rate	$4.392 \text{ min}^{-1}$
5	$k_D$	maximum Dyn secretion rate	$218.047 \text{ nM min}^{-1}$
6	$k_N$	maximum NKB secretion rate	$32.33 \text{ nM min}^{-1}$
7	$p_v$	maximum strength of synaptic inputs	$2.3 \cdot 10^{-3} \text{ min}$
8	$v_0$	maximum rate of neuronal activity increase	$13176 \text{ spikes min}^{-2}$
9	$K_D$	Dyn IC50	0.3 nM
10	$K_N$	NKB EC50	2.991 nM
11	$K_{v,1}$	firing rate for half-maximal Dyn secretion	$810.637 \text{ spikes min}^{-1}$
12	$K_{v,2}$	firing rate for half-maximal NKB secretion	$116.09 \text{ spikes min}^{-1}$
13	$I_0$	basal synaptic inputs	0.0136 (dimensionless)
14	$n_1, n_2, n_3, n_4$	Hill coefficients	2 (dimensionless)
15	$\bar{c}$	synapse probability	0.5
16	$A$	adjacency matrix ( $M \times M$ )	$\text{Prob}(A_{ij} = 1) = \bar{c}$

characteristics, i.e., maximum response amplitude, amplitude of oscillations and the period of oscillation, were calculated from the response trajectory after discarding the first 1000 min.

**Table 2.** Parameter ranges used in the global sensitivity analysis.

No.	Parameter (units)	max. Value	min Value	Distribution
1	$k_D$ (nM)	400	0.4	$\log_{10}$ uniform
2	$k_N$ (nM)	40	0.04	$\log_{10}$ uniform
3	$I_0$ (dimensionless)	0.1	0.0001	$\log_{10}$ uniform

## Supporting information

S1 text. Supporting Information.

## Acknowledgments

KTA and MV gratefully acknowledge the financial support of the EPSRC via grant EP/N014391/1.



## References

1. Herbison AE. Control of puberty onset and fertility by gonadotropin-releasing hormone neurons. *Nature Reviews Endocrinology*. 2016;12(8):452–466. doi:10.1038/nrendo.2016.70.
2. de Roux N, Genin E, Carel JC, Matsuda F, Chaussain JL, Milgrom E. Hypogonadotropic hypogonadism due to loss of function of the KiSS1-derived peptide receptor GPR54. *Proceedings of the National Academy of Sciences*. 2003;100(19):10972–10976. doi:10.1073/pnas.1834399100.
3. Seminara SB, Messenger S, Chatzidaki EE, Thresher RR, Acierno Jr JS, Shagoury JK, et al. The GPR54 Gene as a Regulator of Puberty. *New England Journal of Medicine*. 2003;349(17):1614–1627. doi:10.1056/NEJMoa035322.
4. Kaiser UB. Understanding reproductive endocrine disorders. *Nature Reviews Endocrinology*. 2015;11(11):640–641. doi:10.1038/nrendo.2015.179.
5. Hrabovszky E. Neuroanatomy of the Human Hypothalamic Kisspeptin System. *Neuroendocrinology*. 2014;99(1):33–48. doi:10.1159/000356903.
6. Clarkson J, D'Anglemont de Tassigny X, Colledge WH, Caraty A, Herbison AE. Distribution of Kisspeptin Neurons in the Adult Female Mouse Brain. *Journal of Neuroendocrinology*. 2009;21(8):673–682.
7. Plant TM, Zeleznik AJ. *Knobil and Neill's physiology of reproduction*. Academic Press; 2014.
8. Lehman MN, Coolen LM, Goodman RL. Minireview: Kisspeptin/Neurokinin B/Dynorphin (KNDy) Cells of the Arcuate Nucleus: A Central Node in the Control of Gonadotropin-Releasing Hormone Secretion. *Endocrinology*. 2011;doi:10.1210/en.2010-0022.
9. Kinsey-Jones JS, Li XF, Luckman SM, O'Byrne KT. Effects of Kisspeptin-10 on the Electrophysiological Manifestation of Gonadotropin-Releasing Hormone Pulse Generator Activity in the Female Rat. *Endocrinology*. 2008;149(3):1004–1008. doi:10.1210/en.2007-1505.

10. Navarro VM, Gottsch ML, Chavkin C, Okamura H, Clifton DK, Steiner RA. Regulation of Gonadotropin-Releasing Hormone Secretion by Kisspeptin/Dynorphin/Neurokinin B Neurons in the Arcuate Nucleus of the Mouse. *The Journal of Neuroscience*. 2009;29(38):11859–11866. doi:10.1523/JNEUROSCI.1569-09.2009.
11. Wakabayashi Y, Nakada T, Murata K, Ohkura S, Mogi K, Navarro VM, et al. Neurokinin B and Dynorphin A in Kisspeptin Neurons of the Arcuate Nucleus Participate in Generation of Periodic Oscillation of Neural Activity Driving Pulsatile Gonadotropin-Releasing Hormone Secretion in the Goat. *The Journal of Neuroscience*. 2010;30(8):3124–3132. doi:10.1523/JNEUROSCI.5848-09.2010.
12. Kinsey-Jones JS, Grachev P, Li XF, Lin YS, Milligan SR, Lightman SL, et al. The Inhibitory Effects of Neurokinin B on GnRH Pulse Generator Frequency in the Female Rat. *Endocrinology*. 2011;153(1):307–315. doi:10.1210/en.2011-1641.
13. Sandoval-Guzmán T, E Rance N. Central injection of senktide, an NK3 receptor agonist, or neuropeptide Y inhibits LH secretion and induces different patterns of Fos expression in the rat hypothalamus. *Brain research*. 2004;1026(2):307–312. doi:10.1016/j.brainres.2004.08.026.
14. Qiu J, Nestor CC, Zhang C, Padilla SL, Palmiter RD, Kelly MJ, et al. High-frequency stimulation-induced peptide release synchronizes arcuate kisspeptin neurons and excites GnRH neurons. *eLife*. 2016;5:e16246. doi:10.7554/eLife.16246.
15. Clément F, Françoise JP. Mathematical Modeling of the GnRH Pulse and Surge Generator. *SIAM Journal on Applied Dynamical Systems*. 2007;6(2):441–456. doi:10.1137/060673825.
16. Pomerening JR, Sontag ED, Ferrell JE. Building a cell cycle oscillator: hysteresis and bistability in the activation of Cdc2. *Nature Cell Biology*. 2003;5(4):346–351. doi:10.1038/ncb954.
17. Goldbeter A. Computational approaches to cellular rhythms. *Nature*. 2002;420(6912):238–245. doi:10.1038/nature01259.

18. Navarro VM, Castellano JM, McConkey SM, Pineda R, Ruiz-Pino F, Pinilla L, et al. Interactions between kisspeptin and neurokinin B in the control of GnRH secretion in the female rat. *American Journal of Physiology - Endocrinology and Metabolism*. 2011;300(1):E202–E210.
19. Fergani C, Navarro VM. Expanding the role of tachykinins in the neuroendocrine control of reproduction. *Reproduction*. 2017;153(1):R1–R14. doi:10.1530/REP-16-0378.
20. Han SY, McLennan T, Czielesky K, Herbison AE. Selective optogenetic activation of arcuate kisspeptin neurons generates pulsatile luteinizing hormone secretion. *Proceedings of the National Academy of Sciences*. 2015;112(42):13109–13114. doi:10.1073/pnas.1512243112.
21. Campos P, Herbison AE. Optogenetic activation of GnRH neurons reveals minimal requirements for pulsatile luteinizing hormone secretion. *Proceedings of the National Academy of Sciences*. 2014;111(51):18387–18392. doi:10.1073/pnas.1415226112.
22. Clarkson J, Han SY, Piet R, McLennan T, Kane GM, Ng J, et al. Definition of the hypothalamic GnRH pulse generator in mice. *Proceedings of the National Academy of Sciences*. 2017;114(47):E10216–E10223. doi:10.1073/pnas.1713897114.
23. Doedel EJ, Fairgrieve TF, Sandstede B, Champneys AR, Kuznetsov YA, Wang X. AUTO-07P: Continuation and bifurcation software for ordinary differential equations; 2007.
24. Toni T, Welch D, Strelkowa N, Ipsen A, Stumpf MPH. Approximate Bayesian computation scheme for parameter inference and model selection in dynamical systems. *Journal of The Royal Society Interface*. 2009;6(31):187–202. doi:10.1098/rsif.2008.0172.
25. Ruka KA, Burger LL, Moenter SM. Both Estrogen and Androgen Modify the Response to Activation of Neurokinin-3 and  $\kappa$ -Opioid Receptors in Arcuate Kisspeptin Neurons From Male Mice. *Endocrinology*. 2015;157(2):752–763. doi:10.1210/en.2015-1688.

26. Yasuda K, Raynor K, Kong H, Breder CD, Takeda J, Reisine T, et al. Cloning and functional comparison of kappa and delta opioid receptors from mouse brain. *Proceedings of the National Academy of Sciences*. 1993;90(14):6736–6740. doi:10.1073/pnas.90.14.6736.
27. Seabrook GR, Bowery BJ, Hill RG. Pharmacology of tachykinin receptors on neurones in the ventral tegmental area of rat brain slices. *European Journal of Pharmacology*. 1995;273(1-2):113–119. doi:10.1016/0014-2999(94)00681-V.
28. Marino S, Hogue IB, Ray CJ, Kirschner DE. A methodology for performing global uncertainty and sensitivity analysis in systems biology. *Journal of Theoretical Biology*. 2008;254(1):178–196. doi:10.1016/j.jtbi.2008.04.011.